Available online at http://scik.org

J. Math. Comput. Sci. 11 (2021), No. 1, 149-164

https://doi.org/10.28919/jmcs/5110

ISSN: 1927-5307

IMPACT OF CHEMICAL REACTION ON MASS TRANSFER AND MELTING HEAT TRANSFER OF POROUS MHD CASSON FLUID FLOW

B. SHASHIDAR REDDY[1,*], K. SARITHA[2], J. VENKATA MADHU[1]

[1]Department of Science and Humanities, Sreenidhi Institute of Science and Technology, Ghatkesar, Hyderabad, Telangana, 501301, India

[2]Department of Humanities and Sciences, CVR College of Engineering, Mangalpalli, Ibrahimpatnam, Ranga Reddy, Telangana, 501510, India

Abstract: Melting and chemical reaction impacts on heat and mass transfer of MHD Casson fluid flow over a porous stretching surface is examined numerically in this article. The governing partial differential equations are converted by using adequate transformations and the resulting ordinary differential equations are solved numerically using finite difference scheme along with Thomas algorithm. The graphical illustrations are presented for velocity, temperature and concentration distributions. Also Skin friction, Nusselt number and Sherwood number are elucidated for chosen values of various parameters. To validate the numerical method employed, the present results are compared with the existing literature and found to be in good agreement.

Keywords: Casson fluid; melting; chemical reaction; stretching surface; finite difference scheme.

2010 AMS Subject Classification: 76D05.

---

[*]Corresponding author

E-mail address: bsreddy_shashi@yahoo.com

Received October 15, 2020

1. INTRODUCTION

The model developed by Newtonian fluids cannot explain all the various flow characteristics in this modern technology. For this reason, theory of non-Newtonian fluid flow has become significant. As there are numerous applications of these studies such as casting, production of paper, extrusion of polymers. Casson fluid is one among such non-Newtonian liquids which has attracted many scholars due to its applications in drillings techniques, bio-engineering operations and many more. Some important Casson fluids are jelly, tomato sauce, human blood and soon.

Research work on various properties of heat transfer in Newtonian and non- Newtonian liquids can be found in the literature [1, 2, 3]. In consideration of Viscous dissipation, effect of heat flux on non-Newtonian fluid over a porous moving surface was investigated by Kishan and Shashidar [4]. Hayat and Qasim [5] analyzed the impact of thermophoresis on Maxwell fluid flow. Mixed convection with the effects of various parameters on MHD flow is examined by Narayan [6].

The model of the Casson fluid flow was initially represented by Casson [7] to predict the performance of pigment-oil suspensions. The flow of Casson fluid with radiation effects over stretching surface in porous medium was discussed by Pramanik [8]. The reactions of heterogenous/homogeneous in the flow of Casson fluid was explained by Khan et al. [9]. The impact of Soret and Dufour on the flow of Casson fluid was examined by Hayat et al. [10]. The unsteady MHD flow of Casson liquid past a stretching plate considering various parameters was discussed by Aziz and Afify [11]. Eldabe and Salwa [12] investigated the flow of Casson fluid between rotating cylinders. Khalid et al [13] has presented his studies on convective motion of Casson fluid past a oscillating vertical plate. Heat transfer of Casson liquid past a porous rotating plate was analysed by Raju and Sandeep [14]. Mukhopadhyay [15] constructed Unsteady flow of Casson liquid past a stretching surface with suction/injection. Whereas the Unsteady heat transfer flow of Casson liquid past a moving plate was discussed by Mustafa et al. [16].

In MHD, mass transfer plays significant role because of its significance in many scientific approaches such as convective transfer of molecules and atoms. Mass transfer of MHD Casson liquid past a stretching surface was investigated by Bhattacharyya [17]. Influence of suction on

MHD heat mass transfer past a shrinking surface is investigated by Muhamin and Khamis [18].

Melting heat transfer process in non-Newtonain fluids has played significant role because of its applications in thermal engineering such as solidification, recovery of geothermal energy, magma and many more. Melting effects on MHD Williamson nanofluid flow was investigated by Krishnamurthy et al [19]. Prasannakumara et al [20] analysed the phenomenon of melting on MHD Dusty fluid flow past a stretching surface considering the effects of heat absorption/generation and radiation. Impact of melting on MHD flow past a moving plate with radiation was observed by Kalidas [21]. Sarkar [22] shown the influence of melting MHD Casson nanofluid wedge flow. MHD Carreau fluid flow over melting surface is examined by Ramdev et al. [23].

Heat transfer in the presence of radiation has large number of applications in various industrial processes such as Satellites, missiles, space vehicles and soon. Heat and mass transfer with radiation over a moving plate in porous medium was addressed by Makinde [24]. Heat transfer characteristics on the flow of Casson nanofluid over a stretching surface was examined by Ibrahim et al [25].

The past studies reveals that few works exist in the literature presenting the influence of mass transfer on MHD Casson fluid flows. Recently, Fazle and Kalidas [26] presented the melting effects on the MHD flow of Casson fluid over stretching surface. So our present investigation is to fill this gap. The theme of the present study is to extend the effort of Fazle and Kalidas [26]. The present work is to concentrate on heat and mass transfer of MHD Casson fluid flows past a stretching surface. In this study, fluid is considered in porous medium, also melting effects and thermal radiation are included. The equations governing the flow are solved numerically and the impact of prominent parameters is analysed graphically.

2. FORMULATION OF MODEL

Figure 1 depicts the mathematical model of a 2D steady flow of a MHD Casson fluid past a stretching sheet. Here we consider that the sheet is horizontal and linear in the existence of a porous medium also the fluid is melting at a steady rate into a constant property. Cartesian model is preferred such that x-axis is along the surface and y-direction is perpendicular to the sheet and flow is confined to y > 0. The fluid is assumed to be conducting electrically and subjected to applied magnetic field in normal direction. Let $u_w(x) = cx$ be the stretching sheet velocity and the external flow velocity be $u_e(x) = ax$, where c > 0 and a > 0 be the constants. The melting and free stream temperatures of the liquid be taken as T_m and T_∞ accordingly. The constituent equations determining the Casson liquid is represented by:

$$\tau_{ij} = \begin{cases} 2\left(\mu_B + \dfrac{P_y}{\sqrt{2\pi}}\right)e_{ij}, & \pi > \pi_c \\ 2\left(\mu_B + \dfrac{P_y}{\sqrt{2\pi_c}}\right)e_{ij}, & \pi < \pi_c \end{cases} \tag{1}$$

Where $\pi = e_{ij}e_{ij}$, is the deformation rate, π_c is a critical value of the non-Newtonian fluid, P_y is fluid yield stress, e_{ij} is the $(i, j)^{th}$ component of the deformation rate, μ_B is the plastic dynamic viscosity.

Under the above conditions, the equations governing the flow are [26]:

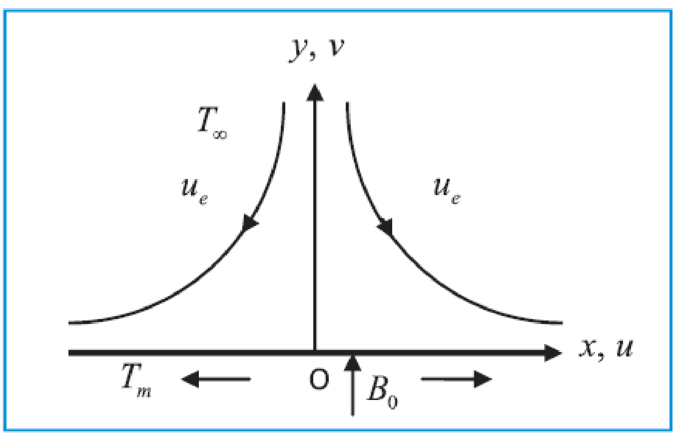

$$\frac{\partial u}{\partial x} + \frac{\partial u}{\partial y} = 0 \tag{2}$$

$$u\frac{\partial u}{\partial x} + v\frac{\partial u}{\partial y} = u_e\frac{du_e}{dx} + \nu\left(1+\frac{1}{\beta}\right)\frac{\partial^2 u}{\partial y^2} - \frac{\sigma B_0^2}{\rho}(u-u_e) - \frac{\nu}{K}(u-u_e) \tag{3}$$

$$u\frac{\partial T}{\partial x}+v\frac{\partial T}{\partial y}=\alpha\frac{\partial^2 T}{\partial y^2}-\frac{1}{\rho C_p}\frac{\partial q_r}{\partial y} \tag{4}$$

$$u\frac{\partial C}{\partial x}+v\frac{\partial C}{\partial y}=D\frac{\partial^2 C}{\partial y^2}-k_1 C \tag{5}$$

Subject to the limit conditions,

$$\begin{aligned} &u=u_w(x)=cx, \quad T=T_m,\ C=C_w \quad at\ \ y=0\\ &u\to u_e(x)=ax,\ T\to T_\infty,\ C\to C_\infty\ as\ \ y\to\infty \end{aligned} \tag{6}$$

And $$k\left(\frac{\partial T}{\partial y}\right)_{y=0}=\rho\left[\lambda+c_s\left(T_\infty-T_0\right)\right]v(x,0) \tag{7}$$

Here K is permeability, u, v are the velocity components, k is thermal conductivity, λ is latent heat α is Thermal diffusivity, ν is kinematic viscosity, ρ is the density of the fluid, β is Casson fluid parameter, c_s is heat capacity, c_p is the specific heat at constant pressure, q_r is radiative heat flux, D is mass diffusion and k_1 is rate of reaction.

Using the approximation of Rosseland [27], we have

$$q_r=-\frac{4\sigma^*}{3k^*}T^3\frac{\partial T}{\partial y} \tag{8}$$

Where σ^* is Stefan-Boltzmann constant, and k^* the absorption coefficient respectively

Using equation (8), equation (4) can be expressed as

$$u\frac{\partial T}{\partial x}+v\frac{\partial T}{\partial y}=\alpha\frac{\partial^2 T}{\partial y^2}-\frac{1}{\rho C_p}\frac{\partial q_r}{\partial y} \tag{9}$$

To transform the equations governing the flow, the following similarity variables are hosted:

$$\eta=y\sqrt{\frac{a}{\nu}}, \quad \psi=x\sqrt{a\nu}\,f'(\eta), \quad \theta(\eta)=\frac{T-T_m}{T_\infty-T_m},\ \ \phi(\eta)=\frac{C-C_\infty}{C_w-C_\infty} \tag{10}$$

Where ψ is the stream function, using which the velocity components are defined as

$$u=\frac{\partial\psi}{\partial y}\ \ and\ v=-\frac{\partial\psi}{\partial x}$$

Then we obtain,

$$u = axf'(\eta), \qquad v = -\sqrt{av}\, f(\eta) \tag{11}$$

Now by means of equation (11), the governing equations are formulated as

$$\left(1+\frac{1}{\beta}\right) f''' + ff'' - f'^{2} + (M+\Omega)(1-f') + 1 = 0 \tag{12}$$

$$(1+R)\theta'' + \Pr f\theta' = 0 \tag{13}$$

$$\phi'' + Scf\phi' - Sc\gamma\phi - KrC = 0 \tag{14}$$

Subject to the boundary conditions:

$$\begin{aligned} &f'(\eta) = \varepsilon,\ \Pr f(\eta) + Me\theta'(\eta) = 0,\ \theta(\eta) = 0,\ \phi(\eta) = 0 && at\ \eta = 0 \\ &f'(\eta) = 0,\ \theta(\eta) = 1,\ \phi(\eta) = 1 && as\, \eta \to \infty \end{aligned} \tag{15}$$

Where, $\beta = \mu_B \dfrac{\sqrt{2\pi_c}}{P_y} \to Casson\ fluid\ parameter$

$M = \dfrac{\sigma B_0^2}{\rho a} \to Magnetic\ parameter$

$\Omega = \dfrac{\nu}{Ka} \to Permeability\ parameter$

$R = \dfrac{16\sigma^* T_\infty^3}{3k^* k} \to Radiation\ parameter$

$\varepsilon = \dfrac{c}{a} \to stretching\ parameter$

$\Pr = \dfrac{\nu}{\alpha} \to \Pr andtl\ number$

$Me = \dfrac{c_p (T_\infty - T_m)}{\lambda + c_s (T_m - T_0)} \to Melting\ paramter$

$Sc = \dfrac{\nu}{D} \to Schmidt\ number$

$\gamma = \dfrac{k_1}{c} \to chemical\ reaction\ parameter$

Expressions of physical quantities such as Skin friction, Nusselt number and Sherwood number are expressed as under:

$$\mathrm{Re}_x^{1/2} C_f = \left(1+\frac{1}{\beta}\right) f''(0) \tag{16}$$

$$\mathrm{Re}_x^{-1/2} Nu_x = -(1+R)\theta'(0) \tag{17}$$

$$\mathrm{Re}_x^{-1/2} Sh_x = -C'(0) \tag{18}$$

Where $\mathrm{Re}_x = \frac{u_e x}{\nu} \rightarrow local\ \mathrm{Re}\,ynolds\ number$

3. NUMERICAL PROCEDURE

The formulated governing equations (12), (13) and (14) are highly non-linear and coupled. Due to this non-linearity and added mathematical difficulties in the process of obtaining the solution has led us to apply numerical method for this model. The influence of diverse parameters will have huge impact on the characteristics of heat and mass transfer. Therefore in this section, numerical solutions for the governing equations subjected to boundary conditions (15) by means of implicit finite difference scheme.

The procedure employed to obtain the numerical solution for the mathematical model is presented as follows:

- Initially, momentum equation is linearized by employing Quasi Linearization Method [28]
- By means of Implicit finite difference scheme, the system of linear Ordinary differential equations is converted to form difference equations
- These algebraic equations are then expressed in matrix-vector form
- Thomas Algorithm is applied to solve this linear system.

As the flow equations are highly non-linear, iteration procedure is employed. In order to carry out the computations, initially equation of momentum is solved to obtain *f(η)*, which is necessary for solving coupled energy equation and mass equations subjected to the boundary conditions employing Thomas algorithm. The numerical values of *f(η)* are assumed as iterative solutions of $(n+1)^{th}$ order and F(η) as the solution of n^{th} order iteration. To check the convergence of the technique, the same program is run for slightly different values of h and no significant changed was noticed in the value. The iterations are repeated until the maximum difference between the present and next iteration values in all the dependent variables satisfy 10^{-5}.

The accuracy of the numerical technique is verified by comparing the values of $f''(0)$ and $\theta'(0)$ for different parametric values with the existing results of Mahood [26] and they are found to be in good agreement.

4. RESULTS AND DISCUSSION:

For the purpose of having rich understanding of the physical model of the problem, a numerical study is performed with the impact of various parameters such as stretching parameter ε, Magnetic parameter M, non-Newtonian Casson fluid parameter β, radiation parameter R, permeability parameter Ω, Prandtl number Pr, melting parameter Me, Schmidth number Sc and chemical reaction parameter k_1 on velocity, temperature and concentration fields which determine the behavior of the fluid flow.

Table 1: Comparison of $f''(0)$ for different values of ε and Me when Pr = 1, M = Ω = R = 0, Sc = 0.1, k_1 = 0, $\beta \to \infty$

	Results of Mahood [26]				**Present Results**			
ε	**Me = 0**	**Me = 1**	**Me = 2**	**Me = 3**	**Me = 0**	**Me = 1**	**Me = 2**	**Me = 3**
0	1.232588	1.037003	0.946851	0.891381	1.248743	1.038628	0.943157	0.885693
0.1	1.146561	0.964252	0.880442	0.828948	1.164316	0.967658	0.878432	0.82483
0.2	1.05113	0.883675	0.806876	0.759752	1.069705	0.888408	0.806249	0.756987
0.5	0.713295	0.599089	0.547021	0.515172	0.729753	0.605187	0.548776	0.515069
1	0	0	0	0	0	0	0	0
2	-1.887307	-1.580484	-1.442747	-1.359211	-1.980601	-1.626101	-1.468287	-1.375376
3	-4.276541	-3.577332	-3.265006	-3.076102	-4.532818	-3.711932	-3.345325	-3.130303

Numerical values of Skin friction, Nusselt number and Sherwood number are computed and presented in the tabular form. Table 1 exhibit that, the impact of melting parameter and stretching parameter is to reduce the skin friction for selected of values of stretching parameter. Whereas melting effect causes enhancement in Nusselt number but it decline with stretching parameter which is evident from table 2. To validate the numerical method a comparative study is done by tabulating the present results along with the existing results [26]. It is observed that the values are in excellent agreement. Also the influence of chemical reaction on the concentration of liquid is studied by computation of Sherwood number for different values of k_1 shown in table 3. It is obvious from the table that the sherwood number raises with the k_1.

Table 2: Comparison of $\theta'(0)$ for different values of ε and Me when Pr = 1, M = Ω = R = 0, Sc = 0.1, k_1 = 0, β→∞

	Results of Mahood [26]		**Present Results**	
ε	**Me=0**	**Me=1**	**Me=0**	**Me=1**
0	-0.570465	-0.361961	-0.559217	-0.364089
0.5	-0.692064	-0.438971	-0.671162	-0.4414
2	-0.979271	-0.621187	-0.92051	-0.620226
5	-1.396355	-0.886425	-1.247393	-0.870098
6	-1.511165	-0.959514	-1.330061	-0.936556

Table 3: Comparison of $\phi'(0)$ for different values of ε and k_1 when Pr = 1, M = Ω = R = 0, Sc = 0.1, Me = 0, β→∞

ε	**k_1 =0**	**k_1 =1**
0	-0.271286	-0.202069
0.5	-0.285227	-0.212885
2	-0.316475	-0.2372
5	-0.358346	-0.269971
6	-0.369019	-0.278353

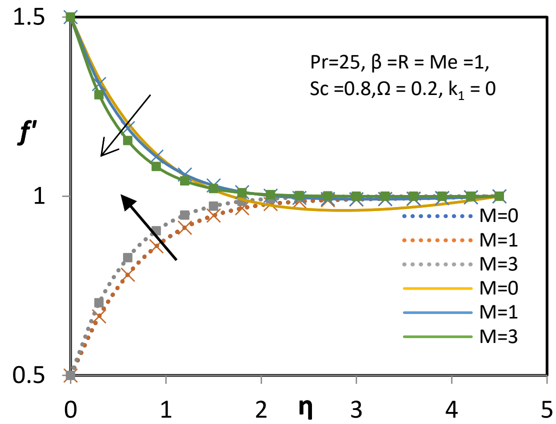

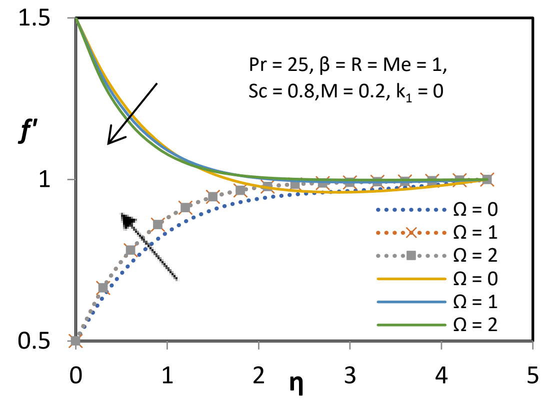

(a) **(b)**

Figure 1: Impact of (a) M and ε (b) Ω and ε on the velocity profiles (……ε = 0.5, ——ε = 1.5)

The impact of magnetic parameter and permeability parameter on velocity distribution is revealed in figure 1. It is clear that the amplitude of the velocity reduces with the escalation in the magnetic parameter. And hence lessening the thickness of velocity boundary layer. It is due to the fact that, when magnetic force is applied normal to the flow, a resistive type of force is generated and by accelerating the magnetic effect, the drag force rises and which decelerates the velocity of the flow. And the outcome of permeability is to reduce the velocity which is shown is figure 1(b). These outcomes are seen when the stretching parameter ε = 1.5, whereas a reverse trend is observed when ε=0.5. Figure 2 elucidates the impact of Casson fluid parameter β and the Prandtl number Pr on velocity profiles for both ε = 1.5 and ε = 0.5. It is evident from the graphs, that fluid motion decreases with β and Pr when ε = 1.5. It is because, as β value is enhanced, the yield stress reduces and the fluid becomes more viscous. Hence the motion of the fluid decelerates. Whereas results are reversed when ε = 0.5. For very large values of β, the fluid totally behaves like a Newtonian fluid. Due to this fact, the thickness of velocity boundary layer is higher for Casson fluid when compared with Newtonian fluids. Similarly, influence of Prandtl number is to reduce the motion of the fluid for ε = 1.5 and velocity rises when ε = 0.5.

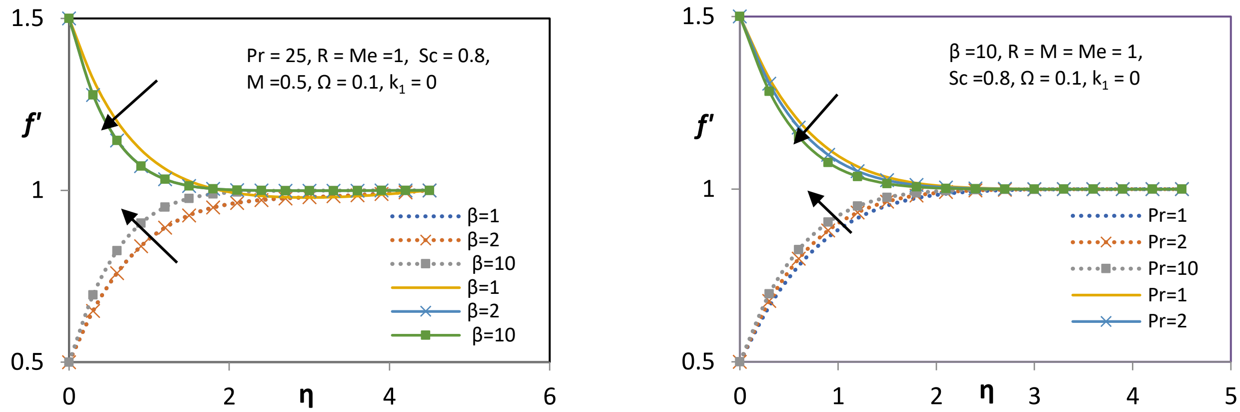

(a) **(b)**

Figure 2: (a) Impact of β and ε (b) Pr and ε on the velocity profiles (……ε = 0.5, ——ε = 1.5)

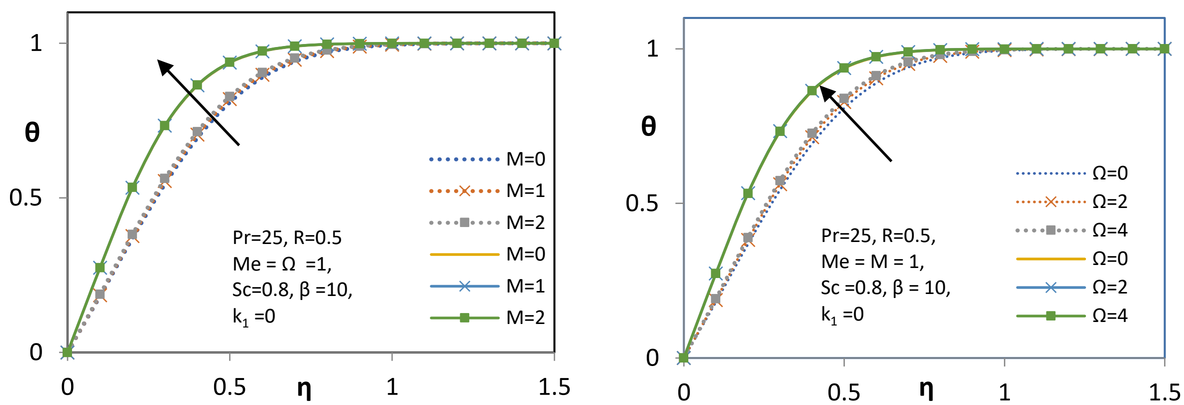

(a) **(b)**

Figure 3: (a) Impact of M and ε (b) Ω and ε on the temperature profiles (…ε = 0.5, ——ε= 1.5)

In Figure 3, the temperature profiles are plotted, for a variety of values of M and Ω keeping other parameters as fixed. It is evident from the figures that, the temperature of the fluid amplifies with the rise in magnetic parameter as well as permeability parameter for both the cases of ε = 0.5 and ε =1.5. This is justified due to the fact the Lorentz force helps to enhance the fluid temperature. The impact of β on temperature distribution is illustrated in figure 4(a). It is evident from the graph that the fluid temperature acts as a growing function of β for both cases ε = 1.5 and ε = 0.5. Correspondingly, the impact of Prandtl number is to enhance the temperature of the Casson fluid for both the cases which is illustrated in figure 4(b).

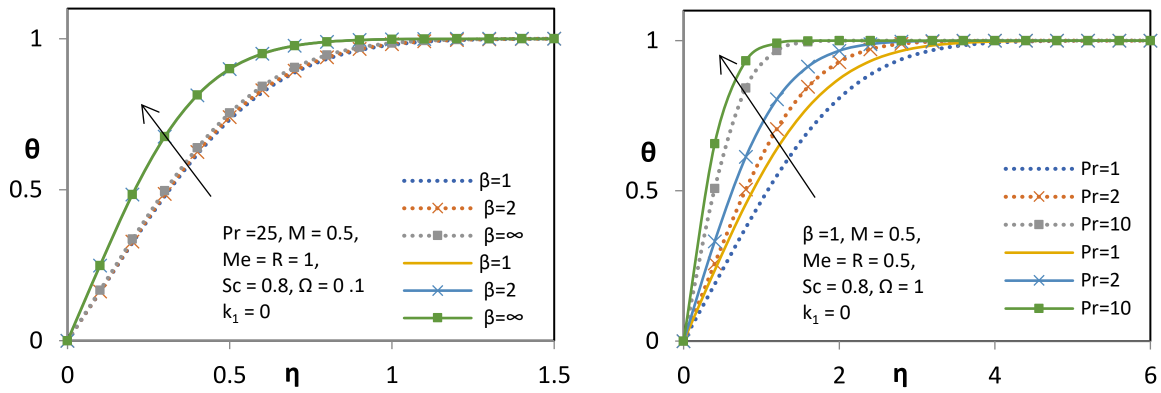

(a) (b)

Figure 4: (a) Impact of β and ε (b) Pr and ε on the temperature profiles (…ε = 0.5, ——ε= 1.5)

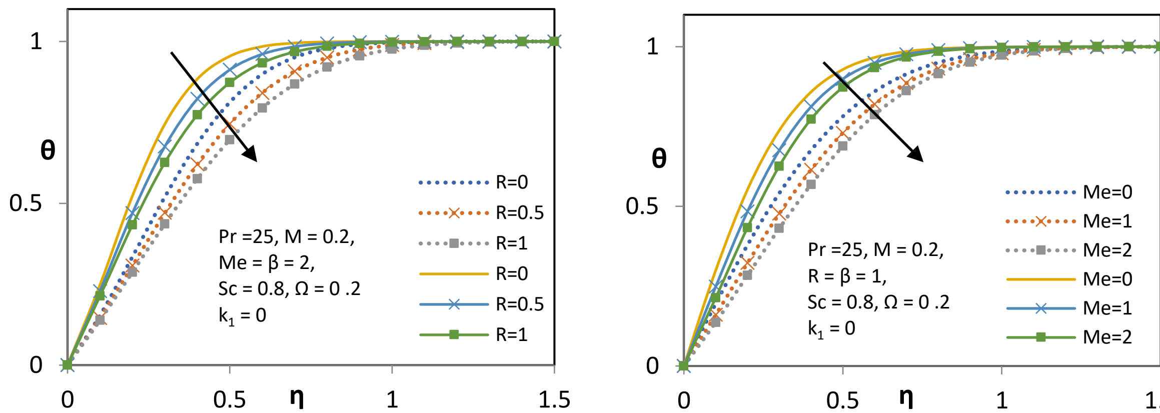

(a) (b)

Figure 5: (a) Impact of R and ε (b) Me and ε on the temperature profiles (…ε = 0.5, ——ε= 1.5)

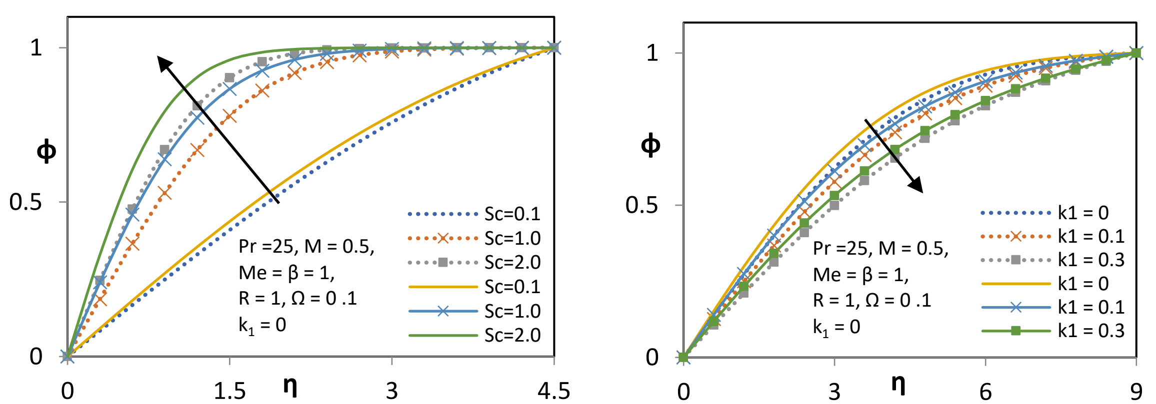

(a) (b)

Figure 6: (a) Impact of Sc and ε (b) k_1 and ε on the concentration profiles (…ε = 0.5, —ε= 1.5)

Figure 5(a) explains the impact of radiation on the fluid temperature on the melting surface. It is illustrated graphically, that the temperature reduces with the increase in radiation parameter. It is due to the reason that radiation enhances the rate of heat transfer on melting surface. And the influence of Melting parameter Me on temperature is sketched in figure 5(b). The temperature of the Casson fluid decreases monotonically from T_m at the surface to T_∞ at infinity. For both the cases of stretching parameter, temperature falls down at the boundary layer. The impact of Schmidt number on concentration profiles is displayed in figure 6(a). Graphical representation shows that concentration profile is increasing function of Sc. Figure 6(b) demonstrates the concentration profiles with the variation of chemical reaction parameter. It is evident from the graph that an increase in the chemical reaction causes reduction in concentration field.

5. CONCLUSIONS:

The development of Casson fluid flow with heat and mass transfer over porous melting stretching surface in the presence of chemical reaction is investigated numerically. The converted flow equations are solved numerically using Finite difference scheme with Thomas algorithm. The influence of various pertinent parameters on velocity, temperature and concentration fields is elucidated graphically. The significant results are listed as follows:

- The impact of magnetic parameter, permeability, Prandtl number and Casson fluid parameter is to decline velocity, accordingly velocity boundary layer thickness reduces.
- Thermal radiation and melting effects tends to depreciate the temperature distribution.
- Temperature of the fluid rises with Magnetic field, permeability, Prandtl number and Casson fluid parameter.
- Schmidt number helps to boost the concentration of the liquid.
- Enhancement in chemical reaction parameter reduces the concentration.
- Impact of melting and stretching parameter is to reduce Skin friction.
- Nusselt number enhances with melting and falls with stretching parameter.
- Sherwood number increases with chemical reaction and decreases with stretching parameter.

CONFLICT OF INTERESTS

The authors declare that there is no conflict of interests.

REFERENCES

[1] C. Fetecau, R. Ellahi, M. Khan, N. A. Shah, Combine porous and magnetic effects on some fundamental motions of Newtonian fluids over an infinite plate, J. Porous Media, 21(7) (2018), 589-605.

[2] A. Zeeshan, N. Ijaz, T. Abbas, R. Ellahi, The sustainable characteristic of Bio-bi-phase flow of peristaltic transport of MHD Jeffery fluid in human body, Sustainability, 10(8) (2018), 2671.

[3] A. Majeed, A. Zeeshan, S.A. Alamri, R. Ellahi, Heat transfer analysis in ferromagnetic viscoelastic fluid flow over a stretching sheet with suction, Neural Comput. Appl. 30(6) (2018), 1947-1955.

[4] Kishan Naikoti, Shashidar Reddy Borra, MHD effects on non-newtonian power-law fluid past a continuously moving porous flat plate with heat flux and viscous dissipation, Int. J. Appl. Mech. Eng. 18 (2013), 425-446.

[5] T. Hayat, M. Qasim, Influence of thermal radiation and Joule heating on MHD flow of a Maxwell fluid in the presence of thermophoresis, Int. J. Heat Mass Transfer, 53 (2010), 4780-4788.

[6] P. V. Satya Narayana, Effects of variable permeability and radiation absorption on magnetohydrodynamic (MHD) mixed convective flow in a vertical wavy channel with traveling thermal waves, Propulsion Power Res. 4(3) (2015), 150-160.

[7] N. Casson, A flow equation forth epigment oil suspensions of the printing ink type, in: C. C. Mills (Ed.), Rheology of Disperse Systems, Pergamon Press, Oxford, New York, 1959.

[8] S. Pramanik, Casson fluid flow and heat transfer past an exponentially porous stretching surface in presence of thermal radiation, Ain Shams Eng. J. 5(1) (2014), 205–212.

[9] M. I. Khan, M. Waqas, T. Hayat, A. Alsaedi, A comparative study of Casson fluid with homogenous-heterogeneous reactions, J. Colloid Interface Sci. 498 (2017), 85-90.

[10] T. Hayat, S. A. Shehzad, A. Alsaedi, Soret and Dufour effects on MHD flow of Casson fluid, Applied Math. Mech.-Engl. Ed. 33 (2012), 1301-1312.

[11] M. A. El-Aziz, A. A. Afify, Effects of Variable Thermal Conductivity with thermal radiation on MHD flow and heat transfer of Casson liquid flim over an Unsteady stretching surface, Brazil. J. Phys. 46 (2016), 516-525.

[12] N. T. M. Eldabe, M. G. E. Salwa, Heat transfer of MHD non-Newtonian Casson fluid flow between two rotating cylinders, J. Phys. Soc. Japan. 64 (1995), 41-64.

[13] A. Khalid, I. Khan, A. Khan, S. Shafie, Unsteady MHD free convection flow of Casson fluid past over an oscillating vertical plate embedded in a porous medium, Eng. Sci. Technol. 18 (2015), 309-317.

[14] C. S. K. Raju, N. Sandeep, Heat and mass transfer in MHD non-Newtonian bio-convection flow over rotating cone/plate with cross diffusion, J. Mol. Liquids, 215 (2016), 115-126.

[15] S. Mukhopadhyay, Effects of thermal radiation on Casson fluid flow and heat transfer over an unsteady stretching surface subjected to suction/blowing, Chin. Phys., B. 22(11) (2013), Article ID 114702.

[16] M. Mustafa, T. Hayat, I. Pop, A. Aziz, Unsteady boundary layer flow of a Casson fluid due to an impulsively started moving flat plate, Heat Transfer Asian Res. 40 (2011), 563-576.

[17] K. Bhattacharyya, T. Hayat, A. Alsaedi, Analytic solution for magnetohydrodynamic boundary layer flow of Casson fluid over a stretching/shrinking sheet with wall mass transfer, Chin. Phys., B. 22 (2013), Article ID 024702.

[18] R. K. Muhaimin, A. B. Khamis, Effects of heat and mass transfer on non-linear MHD boundary layer flow over a shrinking sheet in the presence of suction, Appl. Math. Mech., Engl. Ed. 29(10) (2008), 1309-1317.

[19] M. R. Krishnamurthy, B. C. Prasannakumara, B. J. Gireesha, Rama Subba Reddy Gorla, Effects of Chemical reaction on MHD boundary layer flow and melting heat transfer of Williamson nanofluid in porous medium, Eng. Sci. Technol. 19(1) (2016), 53-61.

[20] B. C. Prasannakumara, B. J. Gireesha, P. T. Manjunatha, Melting Phenomenon in MHD Stagnation point flow of Dusty fluid over a stretching sheet in the presence of thermal radiation and non-uniform heat source/sink, Int. J. Comput. Meth. Eng. Sci. Mech. 16(5) (2015), 265-274.

[21] Kalidas Das, Radiation and melting effects on MHD boundary layer flow over a moving surface, Ain Shams Eng. J. 5 (2014), 1207-1214.

[22] S. Sarkar, M.F. Endalew, Effects of melting process on the hydromagnetic wedge flow of a Casson nanofluid in a porous medium, Bound Value Probl. 2019 (2019), 43.

[23] B. Ramadev, V. Sugunamma, K. A. Kumar, J. V. Ramana Reddy, MHD flow of Carreau fluid over a variable thickness melting surface subject to Cattaneo-Chirstov heat flux, Multidiscipl. Model. Mater. Struct. 15(1)

(2019), 2-25.

[24] O. D. Makinde, Free convection flow with thermal radiation and mass transfer past a moving vertical porous plate, Int. Commun. Heat Mass Transfer, 32 (2005), 1411-1419.

[25] S. M. Ibrahim, P. V. Kumar, G. Lorenzini, F. Mahbood, Numerical study of the onset of chemical reaction and heat source on dissipative MHD stagnation point flow of Casson nanofluid over a nonlinear stretching sheet with velocity slip and convective boundary conditions, J. Eng. Thermophys. 26(2) (2017), 256-271.

[26] Fazal Mabood, Kalidas Das, Outlining the impact of melting on MHD Casson fluid flow past a stretching sheet in a porous medium with radiation, Heliyon, 5(2) (2019), e01216.

[27] S. Rosseland, Astrophysik and atom-theoretische Grundlagen. Springer-Verlag, Berlin, 1931.

[28] R. E. Bellman, R. E. Kalaba, Quasi-Linearization and non-Linear boundary value problems, Elsevier, New York, 1965.